

Organotin complexes with Schiff's base ligands: insights into their cytotoxic effects on lung cancer cells

by Nany Hairunisa FK

Submission date: 18-Aug-2024 02:40PM (UTC+0700)

Submission ID: 2433628163


File name: plexes_with_Schif_s_base_ligands_insights_into_their_artikel.pdf (2.03M)

Word count: 9956

Character count: 49349



Organotin complexes with Schiff's base ligands: insights into their cytotoxic effects on lung cancer cells

Falih Ibadi¹ · Emad Youusif¹  · Ahmed Al-Ani¹ · Mohammed. Al-Mashhadani¹ · Ali Z. Al-Saffar² · Ali Basem³ · Muna Bufaroocha⁴ · Hassan Hashim⁵ · Amani Husain⁶ · Ali H. Jawad⁷ · Nany Hairunisa⁸

Received: 24 April 2024 / Accepted: 18 June 2024
© The Author(s) 2024

Abstract

Organotin(IV) complexes can be used in chemotherapy due to its lipophilicity which can be affected by the availability of Sn coordination bond and bond stabilization between ligand and Sn(IV). In this study, three types of tri-organotin(IV) complexes which are, Ph₃SnL, Me₃SnL, and Bu₃SnL derived from Schiff base ligand were synthesized by the reaction of methyl dithiocarbamate with p-dimethylaminobenzaldehyde. All prepared complexes were characterized using nuclear magnetic resonance (¹H NMR, ¹³C NMR, and ¹¹⁹Sn NMR). The results confirm the coordination of the organotin(IV) moieties to the ligand. The cytotoxicity of tri-organotin(IV) complexes was evaluated against the A549 human lung cancer cell using MTT assay. Ph₃SnL showed a high cytotoxic effect among other complexes, Bu₃SnL also showed a significant cytotoxic effect, while Me₃SnL demonstrated a relatively lower effects. These findings highlight the potential of the tri-organotin(IV) complexes, particularly Ph₃SnL and Bu₃SnL, as promising candidates for further modification as anticancer agents. The results obtained from this study can be used to understand the structure–activity of organotin(IV) complexes and their applications as anti-cancer activity.

Keywords Tri-organotin(IV) complexes · Anti-drugs cancer · MTT assay · A549 human cell · Half-maximal inhibitory concentration (IC50)

1 Introduction

Lung cancer is one of the most lethal malignancies, and it remain a significant health challenge in the world. Therefore the demand to continuous improve the therapeutic agents against cancers still in needed [1, 2]. The organotin(IV) complexes have attracted great attention due to its chemical structures and biological activities [3, 4], and it shows a potential cytotoxic agents against a numerous of cancer cell lines study [5]. In addition, Schiff base ligands have demonstrated a significant ability in the synthesis of different metal complexes [6–8]. These ligands possess versatile coordination abilities and have been utilised in the preparation of organotin(IV) complexes [9]. Many studies have been reported the synthesis and characterization of organotin complexes using Schiff base ligands derived from different aldehydes and amines, and evaluated its activity as anticancer drugs [10]. The biological activity affected by organic groups and the coordination geometry around tin atom [11, 12]. The functional groups of selected ligand can modulate the physicochemical properties of the prepared complexes,

✉ Emad Youusif
emad_yousif@hotmail.com

¹ Department of Chemistry, College of Science, Al-Nahrain University, Baghdad, Iraq

² Department of Molecular and Medical Biotechnology, College of Biotechnology, Al-Nahrain University, Baghdad, Iraq

³ Air Conditioning Engineering Department, Faculty of Engineering, Warith Al-Anbiyaa University, Karbala 56001, Iraq

⁴ Department of Chemistry, College of Science, UAE University, Al-Ain, UAE

⁵ Department of Physics, College of Science, Al-Nahrain University, Baghdad, Iraq

⁶ Polymer Research Unit, College of Science, Mustansiriyah University, Baghdad, Iraq

⁷ Faculty of Applied Sciences, Universiti Teknologi MARA, 40450 Shah Alam, Selangor, Malaysia

⁸ Department of Occupational Medicine, Faculty of Medicine, Universitas Trisakti, Jakarta, Indonesia

which enhance the anti-cancer activity [13]. Therefore, the synthesized organotin(IV) complexes of new Schiff base ligands considered a good candidate for developing of novel anticancer agents. In terms of cytotoxicity evaluation, the MTT (3-(4,5-dimethyl-2-thiazolyl)-2,5-diphenyl-2H-tetrazolium bromide) colorimetric assay is a widely used to assess cell viability and proliferation [14, 15]. This assay depends on the reduction of MTT by mitochondrial enzymes to formazan crystals, which can be measured by spectrophotometer. By measuring the reduction in cell viability caused by the complexes, the cytotoxic effects and its efficacy against cancer cells can be determined. Several studies have been done to study the cytotoxic properties of organotin(IV) complexes against various cancer cell lines [16, 17]. For example, a research done by Abbas et al. (2022) reported the synthesis of novel organotin(IV) complexes with Schiff base ligands and evaluated their cytotoxicity in vitro in silico bio-activities [18]. The results demonstrated a cytotoxic effects and emphasized the potential of these complexes as anti-cancer agents. Moreover, Wang et al. (2022) prepared a different of organotin(IV) complexes with Schiff base ligands and tested their cytotoxic activities against human lung cancer cells [19]. The complexes exhibited a significant cytotoxicity, demonstrating their potential as anti-lung cancer. Based on the studies done before, organotin(IV) complexes derived from Schiff base ligands considered one of the most important drug to be used as anticancer agent [20, 21]. However, further study needed to explain the structure–activity and optimize the design of these complexes to enhance its efficacy in this field. In this study, we synthesized and characterized different organotin(IV) complexes structures derived from Schiff base compounds to assessed its activity against lung carcinoma epithelial cells (A549 cell line).

2 Experimental part

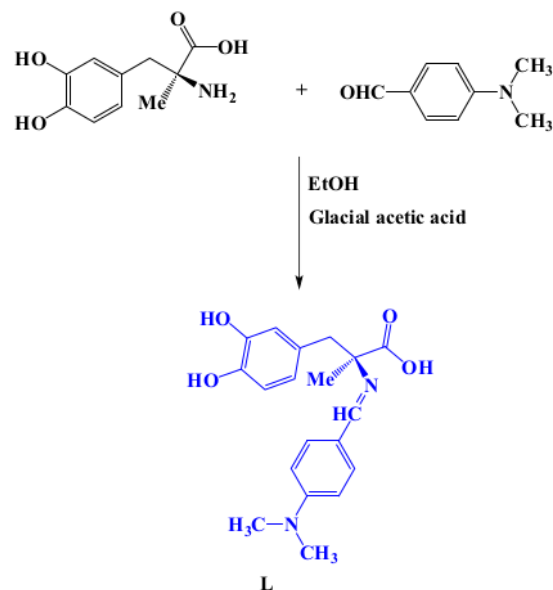
2.1 Chemicals

Methyl dopa was purchased from Scharlau Company, while ethanol, methanol, glacial acetic acid, organotin compounds and para-dimethylaminobenzaldehyde were obtained from Fluka.

2.2 Characterization

2.2.1 Fourier transform infrared spectroscopy (FTIR)

FTIR spectrometer equipped with an attenuated total reflectance (ATR) accessory (ALPHA II Compact FTIR Spectrometer Bruker) was used in the range (4000–400 cm^{-1}) to provide information about functional groups and molecular



Scheme 1 Synthesis of Schiff base ligand (L)

structure by analyze the absorption bands and transmission of infrared light.

2.2.2 Nuclear magnetic resonance (NMR)

NMR spectroscopy (Bruker) was used to provide information about the chemical structure and connectivity of atoms.

2.2.3 Scanning electron microscopy (SEM)

SEM quanta 450 (FEI, USA) was used to get image of the surface morphology and microstructure of samples.

2.2.4 Energy-dispersive X-ray spectroscopy (EDX)

EDS is an elemental analysis to identify the compositions of different elements in a specific sample that combines SEM with X-ray spectroscopy.

2.3 Synthesis of Schiff base ligand (L) [22]

A Schiff base was prepared by dissolving 0.25 g (0.1 mol) of methyl dopa and 0.164 g (0.1 mol) of para-dimethylaminobenzaldehyde in 15 mL of ethanol. The mixture was stirred until all dissolve. To catalyze the reaction, 3 drops of glacial acetic acid were added, and the mixture was refluxed for 3 h as shown in Scheme 1. During this period, a yellow precipitate of Schiff base ligand (L) was formed. Then the reaction mixture was cooled down to room temperature and

Iterate to get the crude product as yellow-white powder. The crude product was recrystallized twice from ethanol to produce pure target product which was used for further characterization and applications.

2.4 Reaction of Schiff base ligand (L) and organotin(IV) complexes

A 0.20 g of synthesized Schiff base ligand was reacted with Ph_3SnCl (0.22 g), Bu_3SnCl (0.20 g), and Me_3SnCl (0.11 g) using 1:1 metal/ligand. The mixtures were refluxed for 6 h at 65 °C in 15 ml methanol as shown in Fig. 2 [23]. The final solutions were filtered, then washing, drying, and recrystallization, to produce Ph_3SnL , Bu_3SnL , and Me_3SnL complexes as off-white powders (Scheme 2). The physical properties of ligand and synthesized organotin complexes are listed in Table 1.

2.5 Cell cultures study

Lung Carcinoma Cells (A549 cell line) was cultured in RPMI-1640 medium with HEPES supplemented with 10% fetal bovine serum (FBS) and 1% penicillin–streptomycin antibiotic and incubated at 37°C in CO_2 (5%) incubator [24]. When cells reached 80–90% confluency, cells were subcultured into new cell culture dishes using the new 49 MI-1640 medium (every 2–3 days). The cell line was provided by the Biotechnology Research Center/Al-Nahrain University.

2.6 In vitro cytotoxicity

The cytotoxic potentials of synthesized tri-organotin (IV) complexes were assessed using MTT assay against A549 cells. An aliquot of 200 μL of A549 cells was maintained in 96-well bottom-flat culture plate at a density of 1×10^5

Table 1 The synthesized organotin complexes' physical characteristics

Compounds	Color	Melting point °C	Yield %
L	White	266–268	81
Ph_3SnL	Off white	290–292	84
Me_3SnL	Off white	294–296	82
Bu_3SnL	Off white	297–299	80

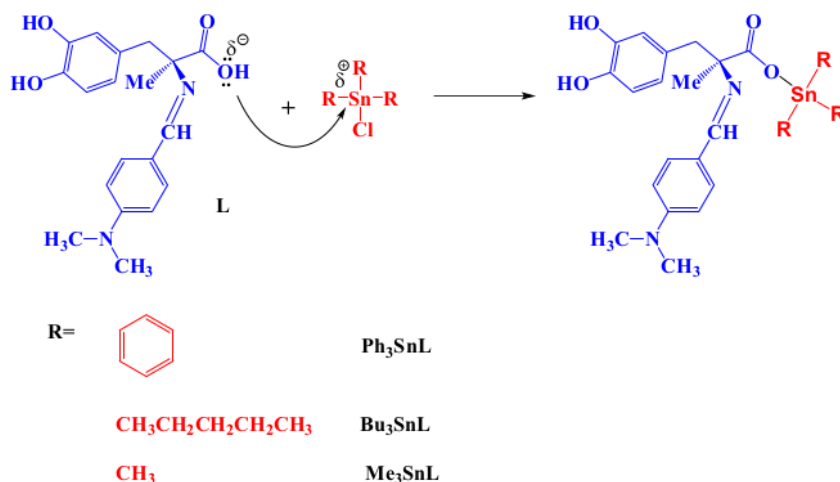
cells/mL. Cells were incubated for 24 h to allow the cells to attach and reach the log phase at the time of tri-organotin (IV) complexes exposure. After incubation, cells were treated with a concentrations of (8, 16, 32, 64, 125, 250, 500 and 1000 $\mu\text{g}/\text{mL}$) of the synthesized complexes for 24 h. After incubation, the medium was removed, and cells were labeled with 538 of MTT solution (5 mg/mL in phosphate buffer saline) for 4 h at 37°C. The resulting formazan was solubilized with 100 μL dimethyl sulfoxide. Incubation was 18 continued for further 10 min and absorbance was measured at 570 nm using a microtiter plate reader (Bio-Rad, USA). The viability of A549 cells was expressed as a percentage of the value for control value according to the below equation and IC_{50} was calculated for each complex depending on viability data [25].

$$\text{Cell Viability (\%)} = \frac{\text{Sample A570}}{\text{Control A570}} \times 100\%$$

2.7 Statistical analysis

18 Statistical analysis was performed using GraphPad Prism version 39.2 (GraphPad Software Inc., La Jolla, CA) to estimate the effect of variable factors on the main study [26]. One-way ANOVA (Tukey Test) was used to determine whether group variance was significant or not. Data were

Scheme 2 Synthesis of the tri-organotin complexes with proposed mechanism



expressed as mean \pm standard deviation and statistical difference was considered at the level of $p < 0.05$.

2.8 Characterization of synthesized organotin(IV) complexes

2.8.1 Scanning electron microscopy (SEM)

SEM was utilized to provide a valuable information about the surface morphology and surface structures of synthesized complexes [27]. Sample prepared by mounted a small amount of ligand and complexes onto a sample holder and sputter-coated with a thin layer of conductive material, such as gold, to improve the conductivity and minimize charging effects during imaging. The SEM images of the ligand was uniform and well-defined particles with surface features, indicating its crystalline nature and regular

crystal growth as shown in Fig. 1. The morphology of the ligand appeared to be in the form of amorphous and microcrystalline structures, which showed a characteristic shape and size distribution.

While the SEM image of organotin(IV) complexes showed different particle size and surface texture, indicating the effect of the coordination of Schiff base ligand with organotin(IV) moieties as shown in Fig. 1. These changes in surface morphology may suggest the formation of larger aggregates or the presence of new surface features resulting from the coordinated bonds. In general, SEM analysis of the ligand and its complexes provide a valuable evidence about the surface characteristics and morphological features. This characterization technique added other analytical methods and contributed to a comprehensive understanding of the complexation of ligand and organotin(IV) complexes.

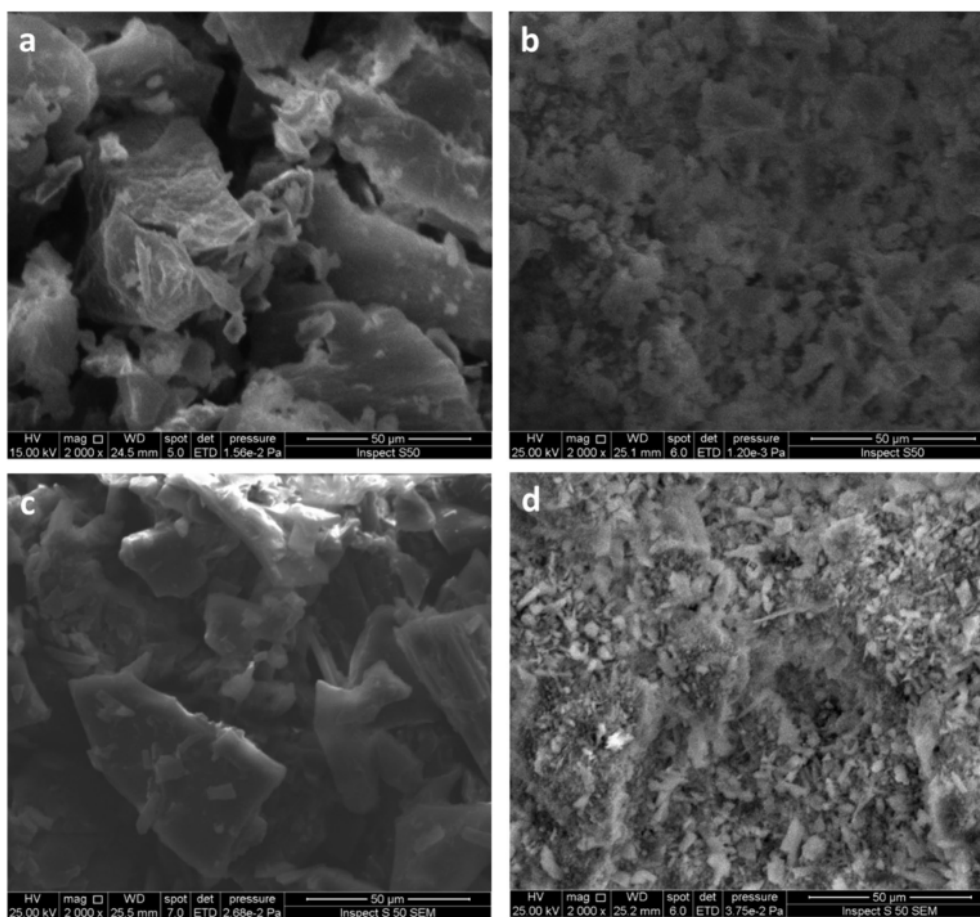


Fig. 1 SEM images of a Ligand (L), b Ph_3SnL complex, c Bu_3SnL complex, and d Me_3SnL complex

2.8.2 Energy dispersive X-ray (EDX)

EDX was used to provide the elemental composition of the prepared complexes. EDX analysis allows the identification and quantification of elements exist in the ligand and synthesised complexes based on their characteristic X-ray emission spectra. A small amount of the samples were mounted on a sample holder, and the EDX detector was positioned to capture the X-ray emissions generated by the interaction of the sample with an electron beam. The detector measures the energy and intensity of the X-rays emitted by the elements present in the prepared samples [28].

EDX analysis of the ligand provided an information about the elements constituting the ligand molecule. The spectrum obtained revealed the presence of carbon, hydrogen, nitrogen, and oxygen, which are typically found in synthesized organic compound (L) as shown in Fig. 2. The relative intensities of the peaks in the spectrum provide insights into the stoichiometry of the synthesized ligand. In the case of the organotin(IV) complexes, EDX analysis confirm the presence of tin (Sn) along with the elements identified in the ligand spectrum as shown in Fig. 2. The relative intensities of the tin peaks compared to the ligand peaks indicated the successful coordination of the ligand with the tin atom in the complexes. The existence of additional elements in the EDX spectrum could provide information about other possible impurities or elements obtained during the synthesis.

29

2.8.3 Fourier transform infrared spectroscopy (FTIR)

FTIR was utilized to provide information about the functional groups exist in the prepared complexes by measuring the absorption of infrared by the molecules [29]. The specific band at 3469 cm^{-1} , indicates the presence of O–H stretching, and the bands at 3097 cm^{-1} and 2926 cm^{-1} were assigned to aromatic C–H stretching, while the band at 1636 cm^{-1} indicated the presence of C=O group. In addition, a band at 1592 cm^{-1} assigned to the presence of C=N of Schiff bases.

For the Ph_3SnL complex, the FTIR showed similar bands as the ligand, with a small shifts. The O–H stretching bands recognised at 3469 cm^{-1} , while the C–H stretching aromatic was at 3098 cm^{-1} . The C–H stretching aliphatic were observed at 2922 cm^{-1} . The C=O band was at 1640 cm^{-1} , and the C=N observed at 1589 cm^{-1} . A new bands were appeared at 527 cm^{-1} and 453 cm^{-1} , confirming the presence of Sn–C and Sn–O bonds in the complex. The FTIR of Bu_3SnL complex showed bands attributed to the ligand's functional groups [30]. The O–H stretching band observed at 3472 cm^{-1} , while the C–H stretching aromatic observed at 3097 cm^{-1} . The aliphatic C–H stretching were appeared as a very sharp and strong bands at 2956 cm^{-1} and 2921 cm^{-1} . The C=O and C=N bands gave two bands at 1637

cm^{-1} and 1598 cm^{-1} respectively. The presence of Sn–C and Sn–O bonds were confirmed by specific bands at 525 cm^{-1} and 451 cm^{-1} respectively. The FTIR of Me_3SnL complex showed O–H stretching band at 3380 cm^{-1} , while the aromatic C–H stretching gave band at 3095 cm^{-1} . The aliphatic C–H stretching were appeared at 2940 cm^{-1} . The C=O and C=N bands appeared at 1636 cm^{-1} and 1590 cm^{-1} respectively. While, bands at 527 cm^{-1} and 452 cm^{-1} confirmed the presence of Sn–C and Sn–O bonds in the formation of the complexes [31]. All FTIR data for synthesized ligand and corresponding complexes were summarized in Table 2.

41

2.8.4 Nuclear magnetic resonance ($^1\text{H-NMR}$)

The $^1\text{H-NMR}$ spectrum of the synthesized Schiff base ligand (L) provides detailed information about its structural features and chemical environments as shown in Fig. 3 [32]. $8.43\text{ (s, 1H, N=CH)}$, this peak corresponds to the proton of the imine group (N=CH), indicating the formation of the Schiff base. The singlet (s) nature of the peak suggests that this proton is not coupled to any nearby protons. 8.02 (s, 1H, OH) and 7.82 (s, 1H, OH) , these peaks correspond to the hydroxyl (OH) protons, indicating the presence of two hydroxyl groups in the Schiff base. The singlet nature of these peaks suggests that these protons are not coupled to any nearby protons. $7.33\text{ (d, J=8.5 Hz, 2H, Ar)}$ and $6.63\text{ (d, J=8.5 Hz, 2H, Ar)}$, these peaks represent the aromatic (Ar) protons. The presence of a doublet (d) indicates that each of these aromatic protons is coupled to two neighboring protons, resulting in a splitting pattern with a coupling constant of 8.5 Hz . Thus 6.53 (m, 2H, Ar) peak corresponds to two aromatic protons that show a multiplet (m) pattern. The multiplet suggests the presence of different neighboring protons, resulting in multiple splitting patterns. While 6.46 (m, 1H, Ar) peak represents a single aromatic proton that exhibits a multiplet pattern, indicating the presence of various neighboring protons. The influence of aromatic substitution on the chemical shift in proton NMR can be explained by the concept of electronic effects. Electron-donating groups, such as hydroxy or amine groups, can donate electron density to the aromatic ring, which leads to shielding of nearby protons. As a result, these protons experience a lower effective magnetic field and appear at lower chemical shift values as shown in Fig. 3.

10

The peaks at $3.13\text{ (d, J=12.4 Hz, 1H, CH)}$ and $2.95\text{ (d, J=12.4 Hz, 1H, CH)}$ correspond to the methylene (CH_2) protons adjacent to a chiral carbon atom. The presence of two doublet peaks arises due to diastereotopicity. In a chiral molecule, the two protons in the CH_2 group experience different chemical environments, leading to non-equivalent coupling patterns. As a result, they give rise to two separate doublet peaks with a coupling constant of 12.4 Hz . $2.90\text{ (s, 6H, 2CH}_3\text{)}$, this peak represents the methyl (CH_3) groups,

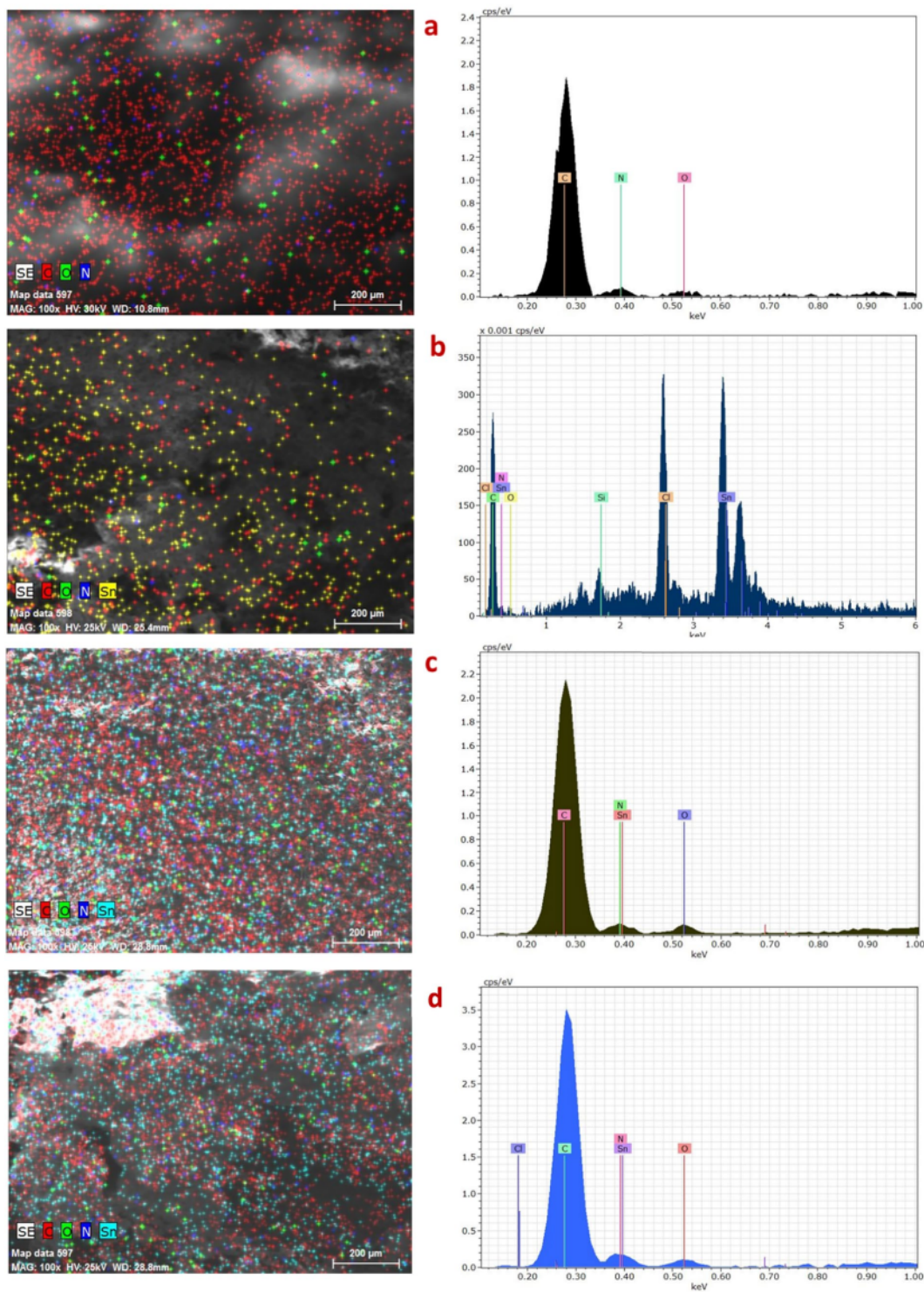
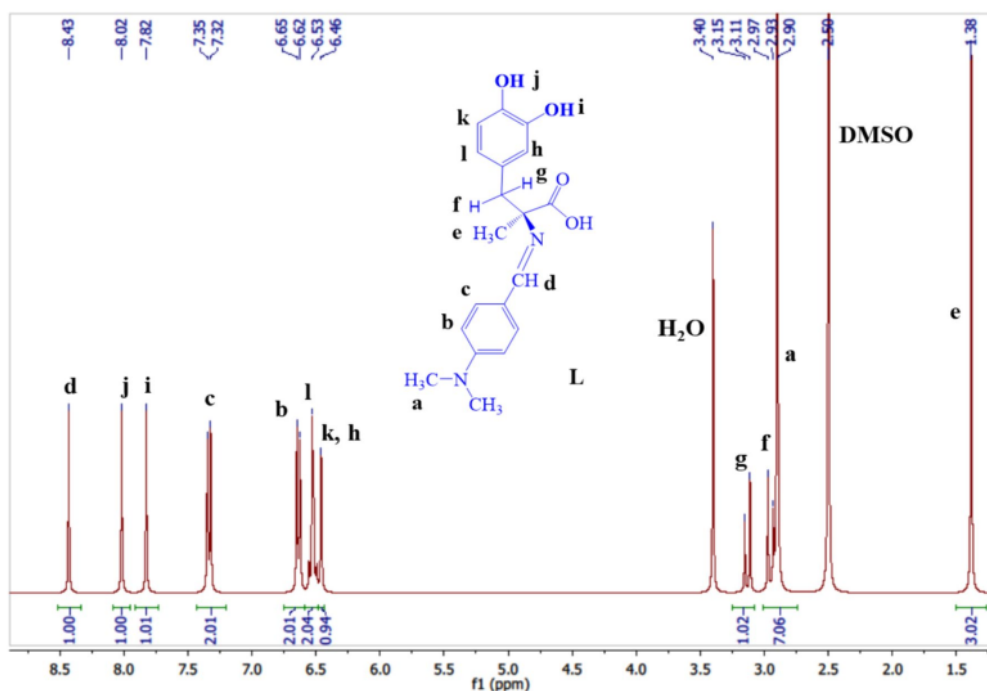


Fig. 2 EDX patterns of a Ligand (L), b Ph₃SnL complex, c Bu₃SnL complex and d Me₃SnL complex

Table 2 FTIR of ligand and complexes

Compounds	Wave number cm^{-1}						
	-OH	C-H Ar	C-H Alph	C=O	C=N	Sn-C	Sn-O
L	3469	3097	2926	1636	1592	-	-
Ph_3SnL	3469–3202	3098	2922	1640	1589	540	453
Bu_3SnL	3472–3199	3097	2956–2921	1637	1598	525	451
Me_3SnL	3380	3095	2940	1638	1590	527	452

**Fig. 3** $^1\text{H-NMR}$ spectrum of ligand

indicating the presence of two methyl groups in the Schiff base. The singlet nature of this peak suggests that these protons are not coupled to any neighboring protons. Finally the peak at 1.38 (s, 3H, CH₃) chemical shift corresponds to the methyl (CH₃) group, indicating the presence of a single methyl group. Similar to the previous case, the singlet nature of this peak suggests that these protons are not coupled to any neighboring protons.

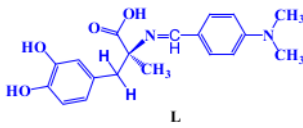
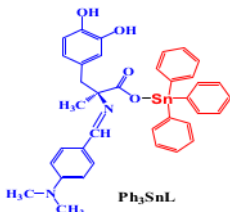
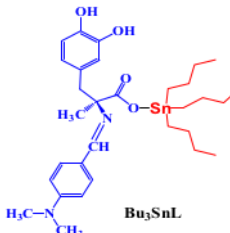
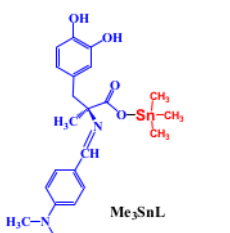
The $^1\text{H NMR}$ analysis of the synthesized Schiff base ligand (L) confirm the presence of different functional groups. The observations of singlets, doublets, multiplets, and diastereotopic splitting patterns support in the identification of specific proton and the characterization of the ligand's structural features. Table 3 summarized the $^1\text{H NMR}$ spectra data for the synthesized ligand and its complexes.

The $^1\text{H NMR}$ spectrum of the synthesized Ph_3SnL complex provides insights into the changes in chemical shifts

compared to the ligand (L) alone. Let's discuss the spectrum in more detail and compare it to the ligand data see Table 3 Fig. 4. The peak at 8.76 (s, 1H, N=CH) corresponds to the proton of the imine group (N=CH) in the complex. The chemical shift is slightly upfield compared to the ligand, indicating a change in the electronic environment due to coordination with the tin atom. Furthermore, the peak at 8.58 (s, 1H, OH) which assigned to the hydroxyl (OH) proton in the synthesized complex. Similarly, the imine group, the chemical shift is slightly upfield compared to the ligand, proposing the effect of the Sn coordination on the electronic field of the OH group. While, the peaks at 7.52–7.30 (m, 1H, OH; 2H, Ar; 15H, 3Ph groups), were assigned to the aromatic protons in the prepared complex. The multiplet (m) pattern indicates the existence of different neighboring protons. The chemical shifts of the aromatic protons show slight variations compared to the ligand, which demonstrate

12

Table 3 $^1\text{H-NMR}$ spectral data for ligand and metal complexes

Compound	$^1\text{H-NMR}$ (400 MHz: DMSO- d_6 , δ , ppm, J in Hz)
 L	8.43 (s, 1H, N=CH), 8.02 (s, 1H, OH), 7.82 (s, 1H, OH), 7.33 (d, $J = 8.5$ Hz, 2H, Ar), 6.63 (d, $J = 8.5$ Hz, 2H, Ar), 6.53 (m, 2H, Ar), 6.46 (m, 1H, Ar), 3.13 (d, $J = 12.4$ Hz, 1H, CH), 2.95 (d, $J = 12.4$ Hz, 1H, CH), 2.90 (s, 6H, 2CH ₃), 1.38 (s, 3H, CH ₃).
 Ph ₃ SnL	8.76 (s, 1H, N=CH), 8.58 (s, 1H, OH), 7.52-7.30 (m, 1H, OH, 2H, Ar, 15H, 3Ph ops), 6.75-6.58 (m, 5H, Ar, from L part), 3.28 (d, $J = 12.4$ Hz, 1H, CH), 3.01 (d, $J = 12.4$ Hz, 1H, CH), 2.90 (s, 6H, 2CH ₃), 1.53 (s, 3H, CH ₃).
 Bu ₃ SnL	8.56 (s, 1H, N=CH), 8.17 (s, 1H, OH), 7.86 (s, 1H, OH), 7.33 (d, $J = 8.5$ Hz, 2H, Ar), 6.68-6.52 (m, 5H, Ar), 3.42 (d, $J = 12.4$ Hz, 1H, CH overlap with H ₂ O peak), 2.99 (d, $J = 12.4$ Hz, 1H, CH), 2.88 (s, 6H, 2CH ₃), 1.59 (s, 3H, CH ₃), 1.45-1.25 (m, 12H, 6CH ₂), 1.12-0.96 (m, 9H, 3CH ₂ , 1CH ₃), 0.66 (m, 6H, 2CH ₃).
 Me ₃ SnL	8.28 (s, 1H, N=CH), 8.03 (s, 1H, OH), 7.87 (s, 1H, OH), 7.28 (d, $J = 8$ Hz, 2H, Ar), 6.72-6.51 (m, 5H, Ar), 3.35 (d, $J = 6$ Hz, 1H, CH), 3.02 (d, $J = 16$ Hz, 1H, CH), 2.89 (s, 6H, 2CH ₃), 1.46 (s, 3H, CH ₃), 1.36 (s, 9H, 3CH ₃).

an impact of Sn coordination on their electronic surroundings. The integration of this peak shows 18 hydrogen atoms 15 of them belongs to the three phenyl groups linked to the tin atom. 6.75–6.58 (m, 5H, Ar, from L part) peaks represent the aromatic protons originating from the ligand portion. The multiplet pattern predict the existence of different adjusting protons. Similarly, the aromatic protons in the prepared complex, the chemical shifts of these protons show slight differences compared to the ligand, which predict a limited impact of Sn coordination. Peaks at 3.28 (d, $J = 12.4$ Hz, 1H, CH) and 3.01 (d, $J = 12.4$ Hz, 1H, CH): were attributed to the methylene (CH₂) protons next to to the chiral carbon atom in the complex. The existence of doublets predict the coupling with one adjacent proton, and the chemical shifts are similar to those in the ligand, proposing that the Sn coordination has a minimal effect on these protons. The peak at 2.90 (s, 6H, 2CH₃), attributed to the methyl (CH₃) groups in the prepared complex. The chemical shift was similar compared to the ligand, demonstrating that the Sn coordination does

not affect the electronic surroundings of these groups. The peak at 1.53 (s, 3H, CH₃), attributed to the methyl (CH₃) group, and the chemical shift as same as the ligand, demonstrating that the Sn coordination has minimal impact on the electronic field of this group.

Generally, the ^1H NMR of the synthesized Ph₃SnL complex shows slight changes in chemical shifts compared to the ligand, which predicting some electronic changes according to the coordination with the Sn atom. On the other hand, the overall structural features and chemical structure of the ligand are conserved in the complex. The aromatic protons and the methylene protons adjacent to the chiral carbon show slight differences in their chemical shifts, which predict an impact of Sn coordination on their electronic surroundings. The -CH₃ groups show no changes, predicting that they are not influenced by Sn atom.

The ^1H NMR analysis of the Bu₃SnL complex gave information about the changes in chemical shifts related to the ligand (L) (Fig. 5). The peak at 8.56 (s, 1H, N=CH) attributed

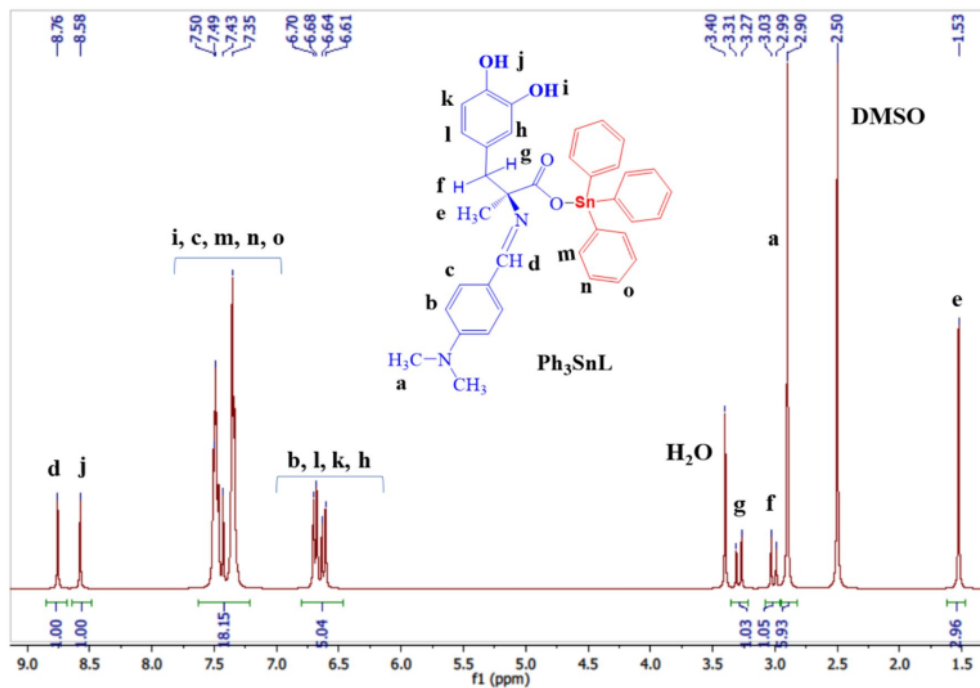


Fig. 4 ¹H-NMR spectrum of Ph₃SnL complex

to the proton of the imine group (N=CH) in the prepared complex. The chemical shift is similar to the ligand, proposing that the electronic fields of this group is slightly affected by the coordination with the butyltin group. While the peak at 8.17 (s, 1H, OH) and 7.86 (s, 1H, OH) assigned to the hydroxyl (-OH) protons in the synthesized complex. The chemical shifts are quite similar to those in the ligand, predicting that the coordination with the butyltin group has negligible effect on the electronic fields of the -OH groups. **37**: peak at 7.33 (d, J = 8.5 Hz, 2H, Ar) attributed to the aromatic protons in the prepared complex.

The existence of a doublet pattern propose coupling with two adjusting protons, and the chemical shift is similar to the ligand, predicting that the Sn coordination has a negligible impact on the electronic field of protons. The peak at 6.68–6.52 (m, 5H, Ar) attributed to the aromatic protons in the complex. The multiplet pattern proposed the presence of different neighboring protons. The chemical shifts are similar to those in the ligand, indicating that the tin coordination does not significantly **30**ect the electronic environment of these protons. 3.42 (d, J = 12.4 Hz, 1H, CH): This peak corresponds to the methylene (CH₂) proton adjacent to the chiral carbon atom in the complex. The presence of a doublet indicates coupling with one neighboring proton. The chemical shift is slightly upfield compared to the ligand,

indicating some electronic modifications upon coordination with the butyltin group. 2.99 (d, J = 12.4 Hz, 1H, CH): This peak represents another methylene (CH₂) proton adjacent to the chiral carbon atom in the complex. The presence of a doublet indicates coupling with one neighboring proton. The chemical shift is comparable to the ligand, suggesting that the tin coordination has minimal influence on the electronic environment of this proton. 2.88 (s, 6H, 2CH₃): This peak represents the methyl (CH₃) groups in the complex. The chemical shift remains unchanged compared to the ligand, indicating that the tin coordination does not significantly affect the electronic environment of these groups. 1.59 (s, 3H, CH₃): This peak corresponds to the methyl (CH₃) group. The chemical shift remains the same as in the ligand, indicating that the tin coordination has minimal influence on the electronic environment of this group. ¹H NMR also showed 1.45–1.25 (m, 12H, 6CH₂), 1.12–0.96 (m, 9H, 3CH₂, 1CH₃), and 0.66 (m, 6H, 2CH₃) peaks represent the CH₂ and CH₃ groups of the three butyl groups linked to tin atom with integration all together 27 hydrogen atom which is exactly represents the butyl groups.

The ¹H NMR spectrum of the synthesized Bu₃SnL complex shows minor changes in chemical shifts compared to the ligand, indicating some electronic modifications upon coordination with the butyltin group. However, the overall

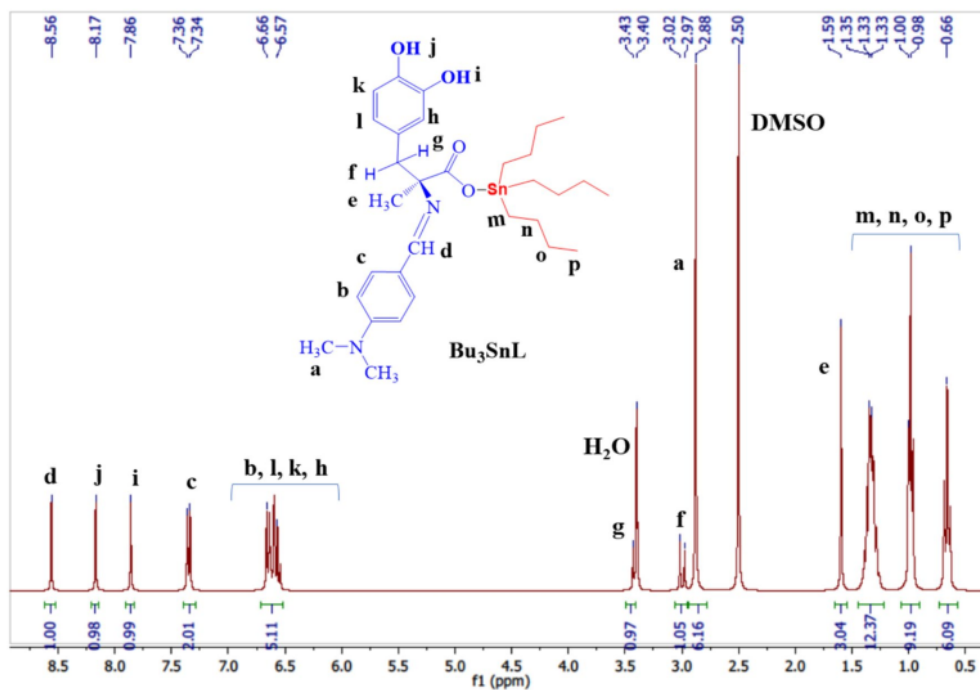


Fig. 5 ^1H -NMR spectrum of Bu_3SnL complex

structural features and chemical environments of the ligand are preserved in the complex. The imine group, hydroxyl groups, aromatic protons, and the methylene groups exhibit chemical shifts similar to those in the ligand, suggesting a limited influence of tin coordination on their electronic environments. But, the methylene proton adjacent to the chiral carbon atom shows a slightly upfield shift, indicating some electronic modifications due to the coordination with the butyltin group.

The ^1H NMR analysis Me_3SnL complex gave changes in chemical shifts related to the ligand (L). The peak at 8.28 (s, 1H, N=CH) corresponds to the imine group (N=CH) proton in the complex. The chemical shift is somewhat downfield compared to the ligand, proposing an electronic change due to coordination with the methyltin group. While the peak at 8.03 (s, 1H, OH) and 7.87 (s, 1H, OH): attributed to the hydroxyl (OH) protons in the complex. The chemical shifts are similar to the ligand, predicting that the coordination with the methyltin group has negligible impact on the electronic field of the -OH group. The peak at 7.28 (d, $J=8$ Hz, 2H, Ar) corresponds to the aromatic protons in the prepared complex. The existence of a doublet indicates coupling with two adjoining protons, and the chemical shift is similar to the ligand, predicting that the Sn coordination does not effect on the electronic field of these protons. Moreover, the peak

at 6.72–6.51 (m, 5H, Ar) represent the aromatic protons in the complex. The multiplet pattern suggests the existence of different adjoining protons. The chemical shifts are similar to those in the ligand, indicating that the Sn coordination has slight effect on the electronic field of protons. Peaks at 3.35 (d, $J=16$ Hz, 1H, CH) and 3.02 (d, $J=16$ Hz, 1H, CH) assigned to the methylene ($-\text{CH}_2$) protons in the complex. The presence of doublets confirms coupling with one adjoining proton, and the chemical shifts are equal to the ligand, proposing that the Sn coordination has a minimal effect on the electronic surroundings of these protons. Furthermore, the peaks at 2.89 (s, 6H, 2CH_3) represents the methyl ($-\text{CH}_3$) groups next to N atom in the complex. The chemical shift remains the same as in the ligand, which indicate the Sn coordination does not influence the electronic environment of these groups. The peak at 1.46 (s, 3H, CH_3) attributed to the methyl ($-\text{CH}_3$) group. The chemical shift is similar to the ligand, which predict that the Sn coordination has a negligible impact on the electronic field of this group. Finally, the peak at 1.36 (s, 9H, 3CH_3): This peak represents the three methyl (CH_3) groups in the complex connected to the Sn atom. In general, the ^1H NMR analysis of the synthesized Me_3SnL complex demonstrate a slight changes in chemical shifts related to the ligand, indicating some electronic changes upon coordination with the methyltin group (Fig. 6).

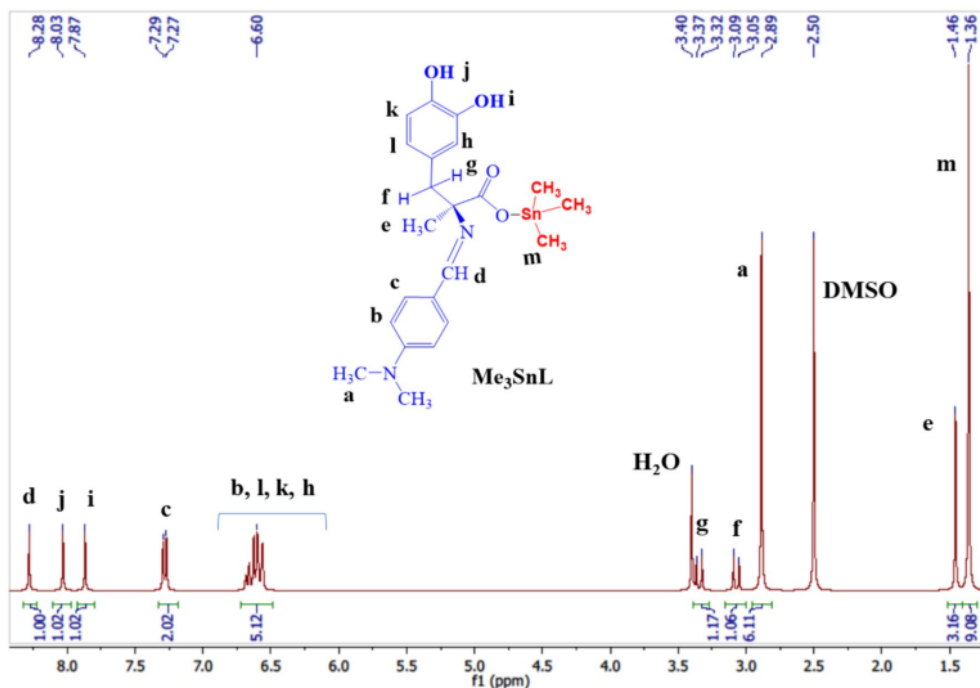


Fig. 6 $^1\text{H-NMR}$ spectrum of Me_3SnL complex

2.8.5 Nuclear magnetic resonance ($^{13}\text{C-NMR}$)

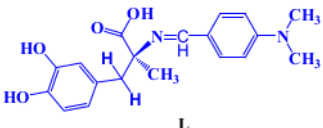
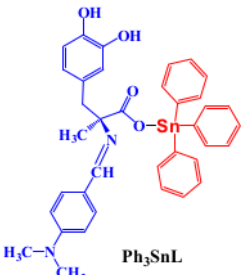
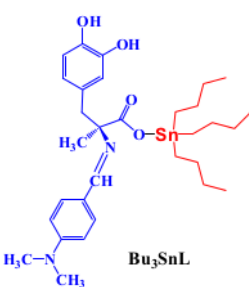
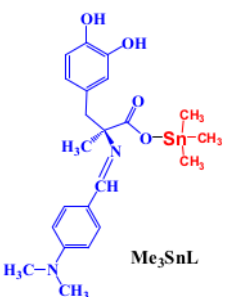
The synthesized ligand (L) and its tin complexes (Ph_3SnL , Bu_3SnL , and Me_3SnL) were characterized using ^{13}C NMR spectroscopy to gain insight into their structural features and confirm the formation of the desired compounds. The ^{13}C NMR spectra provide information about the carbon atoms present in the compounds and their chemical environments. Here is a brief discussion of the results [33, 34].

The ^{13}C NMR spectrum of the ligand (L) would show signals corresponding to the carbon atoms in the methyl dopa and p-dimethylaminobenzaldehyde moieties. The chemical shifts in the ligand spectrum influenced by the substituents and structural arrangement (Table 4). The ^{13}C NMR analysis of the Schiff base gave different peaks, demonstrating the presence of different types of carbon atoms within the ligand structure. The ligand gave peaks at 177.15 and 173.33 ppm, which can be assigned to carbon atoms in carbonyl ($-\text{C}=\text{O}$) and azo-mthine groups ($-\text{C}=\text{N}$). The chemical shifts predict the presence of electron-withdrawing groups or strong deshielding effects on these carbon atoms. A number of peaks in the range of (155.08 – 131.26) ppm indicate the presence of carbon atoms within the aromatic rings. The chemical shifts can vary depending on the substitution and adjusting functional groups. These carbon atoms

in the aromatic rings contribute to the overall aromaticity of the ligand and play a vital role in its chemical features. The chemical shifts at 59.27, 45.39, 41.90, and 21.24 ppm correspond to carbon atoms in aliphatic area, and these carbon atoms are a part of the ligand's backbone or side chains. The differences in the chemical shifts reveal to the differences in the local electronic fields and potential adjusting groups attached to these aliphatic carbon atoms. The detected chemical shifts provide understandings into the ligand's structure and chemical environment. The existence of carbonyl groups proposes the participation of the ligand in coordination chemistry. The aromatic rings is important in the ligand's stability and π -conjugation effects. On the other hand, the aliphatic areas provide information about the contribution to the ligand's solubility and reactivity. Through these results, we can confirm the formation of the compound and gain valuable information about its structural features. These understandings are vital for further studies and the succeeding formation of Sn complexes.

Two peaks observed at 177.15 and 173.33 ppm, which are attributed to carbonyl carbon atoms ($-\text{C}=\text{O}$) and imine ($-\text{C}=\text{N}$) groups of the Schiff base, these peaks undergo a significant downfield shift to 171.41 and 170.95 ppm, respectively in the prepared Ph_3SnL complex. This shift proposes a change in the electronic environment around

Table 4 ^{13}C -NMR spectral of ligand and metal complexes

Compound	^{13}C -NMR (400 MHz: DMSO- d_6 , δ , ppm, J in Hz)
 L	177.15, 173.33, 155.08, 145.47, 144.30, 131.26, 127.04, 122.97, 121.71, 117.97, 117.65, 111.59, 59.27, 45.39, 41.90, 21.24.
 Ph ₃ SnL	171.41, 170.95, 155.08, 145.47, 144.30, 143.45, 134.37, 131.26, 131.03, 129.40, 127.04, 122.97, 121.71, 117.97, 117.65, 111.59, 58.72, 45.13, 41.90, 22.65.
 Bu ₃ SnL	171.41, 170.66, 155.08, 145.47, 144.30, 131.26, 127.04, 122.97, 121.71, 117.97, 117.65, 111.59, 58.72, 45.13, 41.90, 28.55, 24.29, 22.65, 14.01, 10.74.
 Me ₃ SnL	171.82, 171.41, 155.08, 145.47, 144.30, 131.26, 127.04, 122.97, 121.71, 117.97, 117.65, 111.59, 58.72, 45.13, 41.90, 22.65, 1.95.

the carbonyl groups upon coordination to the Sn atom. The peaks detected in the aromatic region of the spectrum (155.08, 145.47, 144.30, 143.45, 134.37, 131.26, 131.03, 129.40, 127.04, 122.97, 121.71, and 117.97 ppm) assigned to carbon atoms of the 's aromatic rings of ligand. These peaks come in accordance Ph₃SnL with the ligand's data, indicating that the coordination of the Sn atom does not significantly change the electronic field of the aromatic rings. The presence of the Sn atom in the Ph₃SnL complex is confirmed by the presence of a peak at 58.72 ppm, which attributed to the carbon atom bonded to Sn atom, and this peak does not appeared in the ligand's spectrum, which indicate

the characteristic feature of the Sn complex. While, the aliphatic group of the Ph₃SnL (45.13, 41.90, and 22.65 ppm) shows peaks that come in accordance with the ligand's data. These peaks represent carbon atoms within aliphatic group of the ligand, prospective part of the ligand's backbone or side chains. Similarly, the chemical shifts suggests that coordination to the Sn atom does not influence the electronic environment of these carbon atoms.

The ^{13}C NMR analysis of Bu₃SnL provides valuable information about the structural features of the synthesized complex. Upon comparison with the ligand, the peaks in the Bu₃SnL spectrum to the ligand's data, several changes

can be observed. These changes provide information of the effects of Sn atom on the ligand's electronic environment. The ligand shows peaks at 177.15 and 173.33 ppm, attributed to the carbonyl carbon atoms ($-C=O$) and imine ($-C=N$) groups in the Schiff base ligand. These peaks show downfield shifts to 171.41 and 170.66 ppm, respectively. This shift proposes a change in the electronic environment around the carbonyl groups upon coordination to the Sn atom. The aromatic area of the spectrum (155.08, 145.47, 144.30, 131.26, 127.04, 122.97, 121.71, and 117.97 ppm) shows peaks that come in accordance with the ligand's data. This indicates that coordination to the Sn atom does not have a significant effect on the electronic environment of the ligand's aromatic rings. The presence of the Sn atom is confirmed by the existence of peak at 58.72 ppm, which is assigned to the carbon atom bonded to the Sn atom. This peak is disappeared in the ligand's spectrum, indicating that it is a characteristic feature of the Sn complex. The aliphatic area of the Bu_3SnL spectrum (45.13, 41.90, 28.55, 24.29, 22.65, 14.01, and 10.74 ppm) also exhibits shifts in chemical shifts compared to the ligand's. These shifts propose changes in the electronic field of the ligand's aliphatic carbon atoms upon coordination with Sn atom. Remarkably, the presence of additional peaks in this region suggests the formation of butyl groups from the tributyltin moiety in the complex.

The ^{13}C NMR analysis of Me_3SnL shows Sn complex formation by Schiff base ligand with trimethyltin chloride (Me_3SnCl), which provides a valuable knowledge of structural changes by Sn coordination. In comparison with the ligand's spectrum, we can investigate the effects of Sn coordination on the ligand's electronic environment. The ^{13}C NMR shows signals corresponding to the ligand carbon atoms, the methyl groups, and the Sn core center. The ligand carbon atoms might behave as a minor chemical shift change due to coordination with Sn atom. Upon analysis of the peaks in the Me_3SnL spectrum and compared to the ligand's data, we can observe several changes in chemical shifts, predicting the impact of Sn coordination on the ligand's structure. Generally, the ligand's spectrum, the presence of carbonyl carbon atoms ($-C=O$) and Schiff base ($-C=N$) groups in the Schiff base are confirmed by peaks at 177.15 and 173.33 ppm. Nevertheless, in the Me_3SnL spectrum, these peaks undergo remarkable higher chemical shifts to 171.82 and 171.41 ppm, respectively.

This suggests that tin coordination induces changes in the electronic environment around the aromatic carbon atoms next to high electronegative atoms such as oxygen and nitrogen. The aromatic region of the spectrum (155.08, 145.47, 144.30, 131.26, 127.04, 122.97, 121.71, and 117.97 ppm) exhibits peaks that align well with the ligand's data, suggesting that the coordination to the Sn atom does not significantly affect the ligand's aromatic rings. The presence of the tin atom in Me_3SnL is confirmed by the appearance of a peak

at 58.72 ppm, corresponding to the chiral carbon atom. In the aliphatic region of the Me_3SnL spectrum (45.13, 41.90, 22.65, and 1.95 ppm), we observe shifts in chemical shifts compared to the ligand's data. These shifts indicate changes in the electronic environment of the ligand's aliphatic carbon atoms due to tin coordination. The appearance of additional peaks in this region suggests the involvement of the methyl groups from the trimethyltin moiety in complex formation. The peak at 1.95 ppm, disappeared in the ligand's spectrum, confirming that it is a characteristic feature of the Sn complex. The ^{13}C NMR spectrum of Me_3SnL demonstrates a significant change in chemical shifts in comparison with the ligand's spectrum, especially for the carbonyl carbon atoms involved in Sn coordination, and the aliphatic carbon atoms affected by the presence of the methyl groups. On the other hand, the aromatic area shows good agreement between the complex and the ligand, indicating a negligible impact on the electronic environment of the ligand's aromatic rings. These results provide valuable insights into the structural and electronic changes induced by tin coordination and contribute to the comprehensive characterization of the complex.

2.8.6 Nuclear magnetic resonance (^{119}Sn -NMR)

The ^{119}Sn NMR analysis provides an essential information about the electronic properties and coordination of Sn complexes, these complexes are, Ph_3SnL , Bu_3SnL , and Me_3SnL . In comparison of the chemical shifts of the Sn atom in these three complexes, we can find the behaviour of the Sn coordinated-ligand and the impact of different organotin groups on the coordination. The ^{119}Sn NMR spectra, showed a chemical shift of the Sn atom in the complexes at -217.31 ppm, -235.57 ppm and -259.57 ppm for Ph_3SnL , Bu_3SnL and Me_3SnL respectively. These chemical shifts are downfield compared to the reference compound, which indicate the effect of the ligand coordination on the electronic surroundings around the Sn atom [35]. The detected downfield shifts in the ^{119}Sn NMR spectra can be attributed to the electronic effects of the different organotin groups and ligand. The ligand, resulting from the Schiff base formation between methyl dopa and p-dimethylaminobenzaldehyde, which contains different functional groups that can contribute to the coordination chemistry with Sn atom. The electron-donating and electron-withdrawing behaviour of these groups can influence the electron density around the ^{119}Sn center, resulting in changes in the ^{119}Sn chemical shifts. By comparing the chemical shifts of the Sn atom in the prepared complexes, we can find the arrangement: Ph_3SnL (-217.31 ppm) $>$ Bu_3SnL (-235.57 ppm) $>$ Me_3SnL (-259.57 ppm). This arrangement proposes that the electronic fields around the Sn atom become more shielded as we move from Ph_3SnL to Bu_3SnL and then to Me_3SnL . This

can be attributed to the changing in electronic properties and steric effects of the different organotin groups.

2.9 Anticancer drugs

2.9.1 Cytotoxic effect of organotin(IV) complexes on A549 human cell

MTT assay can be utilised to evaluate the cytotoxicity of the synthesized tri-organotin(IV) complexes on human lung cancer cells (A549). This assay is based on the ability of living cells to inhibit a yellow tetrazolium salt (MTT) to a purple formazan creation via the activity of mitochondrial dehydrogenases [15, 36]. The colorimetric change reveal the viability of the cells, with a reduction in color that indicating cell death due to apoptosis. In this study, the tri-organotin(IV) complexes and the standard drug doxorubicin were dissolved in acidic medium of isopropanol solvent and diluted with culture medium. Different concentrations (0, 8, 16, 32, 62.5, 125, 250, 500, and 1000 $\mu\text{g}/\text{mL}$) of the complexes and doxorubicin were added to the A549 cells and incubated for 48 h. Then, MTT solution was added and further incubated for 4 h in the dark. The absorbance of the producing formazan was measured at 570 nm.

The inhibition of the tri-organotin(IV) complexes was measured by determining the half maximal inhibitory concentration (IC_{50}). The IC_{50} value represents the concentration of the compounds that inhibits 50% of cell proliferation compared to the normal cells [37]. This parameter gave a valuable information about the influence of the complexes as anti-cancer (Tables 5 and 6). The results can be used to assess the cytotoxicity of the tri-organotin(IV) complexes against human A549 cancer cells. A lower IC_{50} value indicates a higher strength of the complexes to inhibit cell proliferation. The comparison with doxorubicin, as a chemotherapeutic drug, permits for evaluating the relative efficacy of the synthesized complexes in comparison to the standard [38].

The IC_{50} values obtained for the combination of the synthesized Schiff base ligand with different tri-organotin(IV) complexes which found to be 16.84 $\mu\text{g}/\text{mL}$ for Ph_3SnL ,

980.1 $\mu\text{g}/\text{mL}$ for Me_3SnL and 11.63 $\mu\text{g}/\text{mL}$ for Bu_3SnL . The IC_{50} value reflects the concentration of the compounds required to inhibit 50% of cell proliferation compared to untreated cells [39]. In this circumstance, a lower IC_{50} value of (16.84 $\mu\text{g}/\text{mL}$) indicates a higher effectiveness and stronger cytotoxic effect of the compounds on the A549 lung cancer cells. The results demonstrate that the combination of the Schiff base ligand with Ph_3SnL showed the most powerful cytotoxic effect. This suggests a synergistic interaction between the ligand and Sn atom, which enhance a cytotoxic against the A549 cancer cells [40]. On the other hand, the Me_3SnL showed a higher IC_{50} value of (980.1 $\mu\text{g}/\text{mL}$), indicating a less cytotoxic effect associated to the other compounds. This proposes that the communication between ligand and Me_3SnCl may have a weaker synergistic effect on the A549 cells. Similarly, Bu_3SnL exhibited a relatively low IC_{50} value of about (11.63 $\mu\text{g}/\text{mL}$), indicating a significant cytotoxic effect. This indicates that Bu_3SnL possesses a strong cytotoxic properties towards human A549 cancer cells and may give a promise anti-cancer agent. These results gives the ability of tri-organotin(IV) complexes, especially Ph_3SnL and Bu_3SnL , as anti-lung cancer. Further studies are needed to discover their mechanism of action inside the human body to evaluate their activity towards cancer cells, and assess their therapeutic clinically. Statistical analysis and IC_{50} values are shown in Table 7 and Fig. 7.

This indicates its strong potential as an effective anti-cancer agent. Bu_3SnL also showed significant cytotoxicity with an IC_{50} value of 11.63 $\mu\text{g}/\text{mL}$, suggesting its potential as an alternative candidate for further development. Bu_3SnL also showed significant cytotoxicity with an IC_{50} value of 11.63 $\mu\text{g}/\text{mL}$, suggesting its potential as an alternative candidate for further development.

3 Conclusions

In conclusion, tri-organotin(IV) complexes were synthesised by the reaction with Schiff base ligand which produce by the reaction of methyl dopa with p-dimethylaminobenzaldehyde.

Table 5 Effect of complexes and doxorubicin on A549 cells viability

Conc	SB + Ph_3SnL		SB + Me_3SnL		SB + Bu_3SnL	
	Mean	SD	Mean	SD	Mean	SD
1,000	11.79	0.53	49.87	3.50	11.87	0.29
500	13.06	0.59	77.11	3.94	12.55	0.64
250	15.69	2.67	80.59	8.41	14.59	0.29
125	17.73	4.23	90.11	5.07	15.35	1.28
62.5	20.36	5.33	96.51	1.93	17.81	0.44
32	34.27	5.24	96.51	1.93	24.94	5.51
16	59.54	5.95	97.16	1.35	50.98	7.47
8	82.36	11.20	94.29	1.07	86.51	10.11

Table 6 Tukey's multiple comparisons test

Tukey's multiple comparisons test	Below threshold	Summary	Adjusted <i>P</i> value
16			
SB + Ph ₃ SnL vs. SB + Me ₃ SnL	Yes	**	< 0.0001
SB + Ph ₃ SnL vs. SB + Bu ₃ SnL	Yes	*	0.0327
SB + Me ₃ SnL vs. SB + Bu ₃ SnL	Yes	**	< 0.0001
32			
SB + Ph ₃ SnL vs. SB + Me ₃ SnL	Yes	**	< 0.0001
SB + Ph ₃ SnL vs. SB + Bu ₃ SnL	Yes	*	0.0184
SB + Me ₃ SnL vs. SB + Bu ₃ SnL	Yes	**	< 0.0001
62.5			
SB + Ph ₃ SnL vs. SB + Me ₃ SnL	Yes	**	< 0.0001
SB + Ph ₃ SnL vs. SB + Bu ₃ SnL	No	ns	0.7199
SB + Me ₃ SnL vs. SB + Bu ₃ SnL	Yes	**	< 0.0001
125			
SB + Ph ₃ SnL vs. SB + Me ₃ SnL	Yes	**	< 0.0001
SB + Ph ₃ SnL vs. SB + Bu ₃ SnL	No	ns	0.7508
SB + Me ₃ SnL vs. SB + Bu ₃ SnL	Yes	**	< 0.0001
250			
SB + Ph ₃ SnL vs. SB + Me ₃ SnL	Yes	**	< 0.0001
SB + Ph ₃ SnL vs. SB + Bu ₃ SnL	No	ns	0.9397
SB + Me ₃ SnL vs. SB + Bu ₃ SnL	Yes	**	< 0.0001
500			
SB + Ph ₃ SnL vs. SB + Me ₃ SnL	Yes	**	< 0.0001
SB + Ph ₃ SnL vs. SB + Bu ₃ SnL	No	ns	0.9868
SB + Me ₃ SnL vs. SB + Bu ₃ SnL	Yes	**	< 0.0001
1000			
SB + Ph ₃ SnL vs. SB + Me ₃ SnL	Yes	**	< 0.0001
SB + Ph ₃ SnL vs. SB + Bu ₃ SnL	No	ns	0.9996
SB + Me ₃ SnL vs. SB + Bu ₃ SnL	Yes	**	< 0.0001

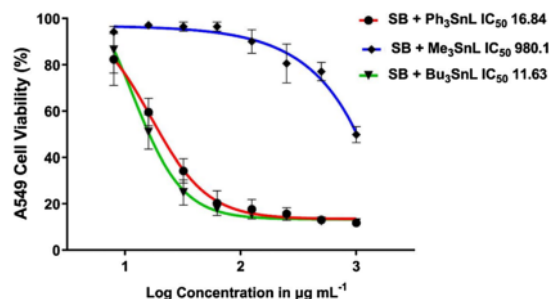
NS non-significant

** *p* < 0.01

* *p* < 0.05

Table 7 Statistical analysis and IC₅₀ values of complexes and doxorubicin

Compound	IC ₅₀ (μg mL ⁻¹)
SB + Ph ₃ SnL	16.84
SB + Me ₃ SnL	980.1
SB + Bu ₃ SnL	11.63

**Fig. 7** Effect of complexes and doxorubicin in mean of A549 cells viability

The characterization of these complexes was acquired by different analysis techniques, such as FTIR, SEM, ¹H NMR, ¹³C NMR, and ¹¹⁹Sn NMR. The resulted spectra gave a valuable information about the structure and coordination of organotin(IV) complexes. The cytotoxicity was evaluated towards A549 human lung cancer cell which demonstrate its activity as anti-cancer agents. The MTT assay shown concentration-dependent growth inhibition of the cancer cells, with Ph₃SnL exhibiting the maximum cytotoxic effect among other synthesized complexes, which confirm by lowest IC₅₀ value (16.84 μg/mL). Bu₃SnL shown a lower cytotoxicity with an IC₅₀ value of (11.63 μg/mL), while Me₃SnL exhibited a relatively lower cytotoxic effect, with an IC₅₀ value of (980.1 μg/mL). The results highlighted the significance of the ligand structure and the behaviour of organotin(IV) complexes. The presence of different organotin(IV) groups have an effect towards anti-cancer agents. The observed cytotoxicity may be attributed to the ability of these complexes to impact with a vital cellular processes or to persuade apoptosis of cancer cells. Further investigations are necessary to demonstrate the mechanisms of action of these complexes, and their selectivity towards cancer cells, and their prospective for combination therapy.

Acknowledgements We thank Al-Nahrain University for technical support.

Author contributions F I, A A, A H and A Z A: experimental work, E Y, M B and N H: conceptualization, M A, A H, Z A and H H: writing—original draft, F I, H H, A B, A H and E Y: review and editing.

Funding No funding was received to assist with the preparation of this manuscript.

Data availability Data is available upon reasonable request from the corresponding author.

1

Declarations

Conflict of interest The authors declare no conflict of interest.

Open Access This article is licensed under a Creative Commons Attribution 4.0 International License, which permits use, sharing, adaptation, distribution and reproduction in any medium or format, as long as you give appropriate credit to the original author(s) and the source, provide a link to the Creative Commons licence, and indicate if changes were made. The images or other third party material in this article are included in the article's Creative Commons licence, unless indicated otherwise in a credit line to the material. If material is not included in the article's Creative Commons licence and your intended use is not permitted by statutory regulation or exceeds the permitted use, you will need to obtain permission directly from the copyright holder. To view a copy of this licence, visit <http://creativecommons.org/licenses/by/4.0/>.

References

- Seebacher NA, Stacy AE, Porter GM, Merlot AM (2019) Clinical development of targeted and immune based anti-cancer therapies. *J Exp Clin Cancer Res* 38(1):156
- Al Talebi Z, Farhood AS, Hadi AG (2023) A comprehensive review of organotin complexes: synthesis and diverse applications. *Cancer Cell* 8:20
- Kumar M, Abbas Z, Tuli HS, Rani A (2020) Organotin complexes with promising therapeutic potential. *Curr Pharmacol Rep* 6:167–181
- Graisa AM, Zainulabdeen K, Salman I, Al-Ani A, Mohammed R, Hairunisa N, Mohammed S, Yousif E (2022) Toxicity and antitumor activity of organotin (IV) compounds. *Baghdad J Biochem Appl Biol Sci* 3(02):99–108
- Hadi AG, Jawad K, Ahmed DS, Yousif E (2019) Synthesis and biological activities of organotin (IV) carboxylates: a review. *Syst Rev Pharm* 10(1):26–31
- Hammoda RG, Shaalan N, Al-Mashhadani MH, Ahmed A, Yusop RM, Bufaroosha M, Yousif E (2023) Design, and synthesis of a plasticizer-Schiff's bases complexes as additive for polystyrene. *J Polym Res* 30(7):265
- Win YF, Yousif E, Ha ST, Majeed A (2013) Synthesis, characterization and preliminary in vitro antibacterial screening activity of metal complexes derivatives of 2-[[5-(4-Nitrophenyl)-1, 3, 4-thiadiazol-2-ylimino] methyl] phenol. *Asian J Chem* 25(8):4203
- Nordin ML, Abdul Kadir A, Zakaria ZA, Othman F, Abdullah R, Abdullah MN (2017) Cytotoxicity and apoptosis induction of *Ardisia crispa* and its solvent partitions against *Mus musculus* mammary carcinoma cell line (4T1). *J Evid Based Complement Altern Med* 16:2017
- Yaseen AA, Al-Tikrity ET, El-Hiti GA, Ahmed DS, Baashen MA, Al-Mashhadani MH, Yousif E (2021) A process for carbon dioxide capture using Schiff bases containing a trimethoprim unit. *Processes* 9(4):707
- Graisa AM, Husain AA, Al-Ani A, Ahmed DS, Al-Mashhadani MH, Yousif E (2022) The organotin spectroscopic studies of hydroxamic as a ligand: a systematic review. *Al-Nahrain J Sci* 25(1):14–23
- Jimaa RB, Al-Zinke JM (2021) A review on organotin (Iv) thiosemicarbazone complexes, synthesis, characterization and biological activity. *J Anbar Pure sci* 15(2):66–73
- Gleeson B, Claffey J, Ertler D, Hogan M, Müller-Bunz H, Paradisi F, Wallis D, Tacke M (2008) el organotin antibacterial and anticancer drugs. *Polyhedron* 27(18):3619–3624
- Alkhamis K, Alatawi NM, Alsoliemy A, Qurban J, Alharbi A, Khalifa ME, Zaky R, El-Metwaly NM (2023) Synthesis and investigation of bivalent thiosemicarbazone complexes: conformational analysis, methyl green DNA binding and in-silico studies. *Arab J Sci Eng* 48:273–290
- Makia R, Al-Sammarrae K, Al-Halbosiy M, Al-Mashhadani M (2022) In vitro cytotoxic activity of total flavonoid from *Equisetum Arvense* extract. *Rep Biochem Mol Biol* 11(3):487
- Ullah H, Previtali V, Mihigo HB, Twamley B, Rauf MK, Javed F, Waseem A, Baker RJ, Rozas I (2019) Structure-activity relationships of new organotin (IV) anticancer agents and their cytotoxicity profile on HL-60, MCF-7 and HeLa human cancer cell lines. *Eur J Med Chem* 181:111544
- Attanzio A, D'Agostino S, Busà R, Frazzitta A, Rubino S, Giraldo MA, Sabatino P, Tesoriere L (2020) Cytotoxic activity of organotin (IV) derivatives with triazolopyrimidine containing exocyclic oxygen atoms. *Molecules* 25(4):859
- Mogharbel AT, Hossan A, Abualnaja MM, Aljuhani E, Pashameah R, Alrefae SH, Abumelha HM, El-Metwaly NM (2023) Green synthesis and characterization of new carbothioamide complexes; cyclic voltammetry and DNA/methyl green assay supported by silico ways versus DNA-polymerase. *Arab J Chem* 16:104807
- Abbas Z, Kumar M, Tuli HS, Janahi EM, Haque S, Harakeh S, Dhama K, Aggarwal P, Varol M, Rani A, Sharma S (2022) Synthesis, structural investigations, and in vitro/in silico bioactivities of flavonoid substituted biguanide: a novel schiff base and its diorganotin (IV) complexes. *Molecules* 27(24):8874
- Wang J, Chen H, Song Q, Liu X, Li C, Wang H, Li C, Hong M (2022) Synthesis and in vitro cytotoxicity study of three diorganotin (IV) Schiff base di-acylhydrazone complexes. *J Inorg Biochem* 236:111983
- Banti CN, Hadjikakou SK, Sismanoglu T, Hadjiliadis N (2019) Anti-proliferative and antitumor activity of organotin (IV) compounds. An overview of the last decade and future perspectives. *J Inorg Biochem* 194:114–152
- Alqahtani AM, Abumelha HM, Alnoman RB, Abualnaja MM, Alsharief HH, Hameed A, Almontshery AM, El-Metwaly NM (2023) Copper (I)-catalysed synthesis of symmetrical perfluoro-terphenyl analogues; fluorescence, antioxidant and molecular docking studies. *Luminescence* 38:1440–1448
- Ahmed AA, Al-mashhadani MH, Hashim H, Ahmed DS, Yousif E (2021) Morphological, color impact and spectroscopic studies of new schiff base derived from 1, 2, 4-triazole ring. *Prog Color Color Coat* 14(1):27–34
- Alhaydary E, Yousif E, Al-Mashhadani MH, Ahmed DS, Jawad AH, Bufaroosha M, Ahmed AA (2021) Sulfamethoxazole as a ligand to synthesize di-and tri-alkyltin (IV) complexes and using as excellent photo-stabilizers for PVC. *J Polym Res* 28(12):469
- Gorry M, Yoneyama T, Vujanovic L, Moss ML, Garlin MA, Miller MA, Herman J, Stabile LP, Vujanovic NL (2020) Development of flow cytometry assays for measuring cell-membrane enzyme activity on individual cells. *J Cancer* 11(3):702
- Jaafar ND, Al-Saffar AZ, Yousif EA (2020) Genotoxic and cytotoxic activities of lantadene A-loaded gold nanoparticles (LA-AuNPS) in MCF-7 cell line: an in vitro assessment. *Int J toxicol* 39(5):422–432
- Mahmood RI, Abbass AK, Al-Saffar AZ, Al-Obaidi JR (2021) An in vitro cytotoxicity of a novel pH-sensitive lectin loaded-cockle shell-derived calcium carbonate nanoparticles against MCF-7 breast tumour cell. *J Drug Delivery Sci Technol* 61:102230
- Awad AA, Hasson MM, faron Alfarhani B. (2019) Synthesis and characterization of a new Schiff base ligand type N₂O₂ and their

- cobalt (II), nickel (II), copper (II), and zinc (II) complexes. *Int J Phys* 1294(5):52040
28. Mehmood N, Andreasson E, Kao-Walter S (2014) SEM observations of a metal foil laminated with a polymer film. *Procedia mater sci* 3:1435–1440
 29. Nikafshar S, Zabihi O, Ahmadi M, Mirmohseni A, Taseidifar M, Naebe M (2017) The effects of UV light on the chemical and mechanical properties of a transparent epoxy-diamine system in the presence of an organic UV absorber. *Materials* 10(2):180
 30. Saleh TA, Al-Tikrity ET, Yousif E, Al-Mashhadani MH, Jawad AH (2022) Preparation of Schiff bases derived from chitosan and investigate their photostability and thermal stability. *Phys Chem Res* 10(4):549–557
 31. Ibrahim M, Nada A, Kamal DE (2005) Density functional theory and FTIR spectroscopic study of carboxyl group. *Indian J Pure Appl Phys* 43:911–917
 32. Mohammed A, Al-Mashhadani MH, Ahmed AU, Kassim MM, Haddad RA, Rashad AA, Al-Dahhan WH, Ahmed A, Salih N, Yousif E (2022) Evaluation the proficiency of irradiative poly (vinyl chloride) films in existence of di- and tri-organotin (IV) complexes. *InAIP Conference Proceedings* 2394(1).
 33. Tcharkhetian AE, Bruni AT, Rodrigues CH (2021) Combining experimental and theoretical approaches to study the structural and spectroscopic properties of flakka (α -pyrrolidinopentiophenone). *Results Chem* 3:100254
 34. Pavia DL, Lampman GM, Kriz GS, Vyvyan JR. (2015) Introduction to spectroscopy.
 35. Hani R, Geanangel RA (1982) ^{119}Sn NMR in coordination chemistry. *Coord Chem Rev* 44(2):229–246
 36. Shaheen F, Ali S, Shahzadi S (2017) Synthesis, characterization, and anticancer activity of organotin (IV) complexes with sodium 3-(1 H-Indol-3-yl) propanoate. *Russ J Gen Chem* 87:2937–2943
 37. Hadi NA, Mahmood RI, Al-Saffar AZ (2021) Evaluation of antioxidant enzyme activity in doxorubicin treated breast cancer patients in Iraq: a molecular and cytotoxic study. *Gene Rep* 24:101285
 38. Brauchle E, Thude S, Brucker SY, Schenke-Layland K (2014) Cell death stages in single apoptotic and necrotic cells monitored by Raman microspectroscopy. *Sci Rep* 4(1):4698
 39. Qiu YR, Zhang RF, Zhang SL, Cheng S, Li QL, Ma CL (2017) el organotin (IV) complexes derived from 4-fluorophenyl-selenoacetic acid: synthesis, characterization and in vitro cytostatic activity evaluation. *New J Chem* 41(13):5639–5650
 40. Guo JR, Chen QQ, Lam CW, Zhang W (2015) Effects of karanjin on cell cycle arrest and apoptosis in human A549, HepG2 and HL-60 cancer cells. *Biol Res* 48:1–7

Publisher's Note Springer Nature remains neutral with regard to jurisdictional claims in published maps and institutional affiliations.

Organotin complexes with Schiff's base ligands: insights into their cytotoxic effects on lung cancer cells

ORIGINALITY REPORT

15%

SIMILARITY INDEX

14%

INTERNET SOURCES

12%

PUBLICATIONS

6%

STUDENT PAPERS

PRIMARY SOURCES

1	pure.sruc.ac.uk Internet Source	2%
2	www.scilit.net Internet Source	1%
3	www.researchgate.net Internet Source	1%
4	biointerfaceresearch.com Internet Source	1%
5	www.mdpi.com Internet Source	1%
6	kups.ub.uni-koeln.de Internet Source	1%
7	paccon2015.kmutt.ac.th Internet Source	<1%
8	anjs.edu.iq Internet Source	<1%
9	Sonia Saroya, Sonika Asija, Naresh Kumar, Yogesh Deswal, Jai devi. "Organotin (IV)	<1%

complexes derived from tridentate Schiff base ligands: Synthesis, spectroscopic analysis, antimicrobial and antioxidant activity", Journal of the Indian Chemical Society, 2022

Publication

10

123dok.org

Internet Source

<1 %

11

www2.mdpi.com

Internet Source

<1 %

12

Submitted to Al-Nahrain University

Student Paper

<1 %

13

Rensheng Xu, Yang Ye, Weimin Zhao.
"Introduction to Natural Products Chemistry",
CRC Press, 2019

Publication

<1 %

14

assets.researchsquare.com

Internet Source

<1 %

15

Jonathan T. Sims. "MTT assays cannot be
utilized to study the effects of STI571/Gleevec
on the viability of solid tumor cell lines",
Cancer Chemotherapy and Pharmacology,
04/26/2009

Publication

<1 %

16

Ravindra S. Shinde, A. K. Haghi. "Modern
Green Chemistry and Heterocyclic
Compounds - Molecular Design, Synthesis,
and Biological Evaluation", CRC Press, 2020

<1 %

17	pastel.archives-ouvertes.fr Internet Source	<1 %
18	jgeb.springeropen.com Internet Source	<1 %
19	sc.nahrainuniv.edu.iq Internet Source	<1 %
20	Chayan Pandya, Akella Sivaramakrishna. "Exploring the binding properties of DNA/BSA and cytotoxicity studies with new terpyridine-ester-based metal complexes (M=Fe(III), Ni(II), Cu(II) and Ru(III)) – A comparative analysis", International Journal of Biological Macromolecules, 2024 Publication	<1 %
21	www.diva-portal.org Internet Source	<1 %
22	www.fedoa.unina.it Internet Source	<1 %
23	www.freepatentsonline.com Internet Source	<1 %
24	Submitted to University of Aberdeen Student Paper	<1 %
25	d-nb.info Internet Source	<1 %

26	lib.buet.ac.bd:8080 Internet Source	<1 %
27	patents.justia.com Internet Source	<1 %
28	www.ijpsonline.com Internet Source	<1 %
29	scholar.lib.vt.edu Internet Source	<1 %
30	Submitted to Flinders University Student Paper	<1 %
31	Submitted to Université Saint-Esprit Kaslik Student Paper	<1 %
32	discovery.ucl.ac.uk Internet Source	<1 %
33	hdl.handle.net Internet Source	<1 %
34	journals.tubitak.gov.tr Internet Source	<1 %
35	Gijsbert van der Marel, Jeroen Codee. "Carbohydrate Chemistry - Proven Synthetic Methods, Volume 2", CRC Press, 2019 Publication	<1 %
36	M. I. Khan, Musa Kaleem Baloch, Muhammad Ashfaq, Saima Gul. "Organotin(IV) esters of 4-	<1 %

maleimido-benzoic acid: synthesis, characterization and in vitro anti-leishmanial effects", Journal of the Brazilian Chemical Society, 2009

Publication

37

Mark E. Thompson. "Electrophosphorescent Materials and Devices", Jenny Stanford Publishing, 2023

Publication

<1 %

38

Ruyan Wan, Xiaohua Xia, Peijin Wang, Weiran Huo, Hui Dong, Zhongjie Chang. "Toxicity of imidazoles ionic liquid [C 16 mim]Cl to HepG2 cells", Toxicology in Vitro, 2018

Publication

<1 %

39

assets-eu.researchsquare.com

Internet Source

<1 %

40

Zeng, Xianhuang. "Divergent Syntheses of Three Indole Alkaloids Classes Enabled by a Tandem Cycloaddition Cascade of 1,3, 4-Oxadiazole", The Scripps Research Institute, 2023

Publication

<1 %

41

pubs.rsc.org

Internet Source

<1 %

42

www.techscience.com

Internet Source

<1 %

43 Nurul Amalina Abd Aziz, Normah Awang, Nurul Farahana Kamaludin, Nur Najmi Mohamad Anuar et al. "The Development of Organotin(IV) N-Ethyl-N-Benzyldithiocarbamate Complexes: A Study on Their Synthesis, Characterization, and Cytocidal Effects on A549 Cell Line", *Anti-Cancer Agents in Medicinal Chemistry*, 2024
Publication

44 Safaa H. Mohamed, Emad Yousif, Ayad S. Hameed, Dina S. Ahmed et al. "Morphology and Performance of PolyVinyl Chloride Thin Films Doped with Polyorganosilanes against Photodegradation", *Silicon*, 2023
Publication

45 Wujiu Jiang, Pengfei Zhou, Le Chen, Weiwei Fu, Yuxing Tan. "Synthesis, crystal structures, and biological activity of aroylhydrazone di-m-chlorobenzyltin complexes", *JBIC Journal of Biological Inorganic Chemistry*, 2023
Publication

46 link.springer.com
Internet Source

47 mdpi-res.com
Internet Source

48 tel.archives-ouvertes.fr
Internet Source

Exclude quotes Off

Exclude matches < 10 words

Exclude bibliography On